Cancer Risk Prediction for Carbon Tetrachloride Using Pharmacokinetic and Cell-Kinetic Models

Kenneth T. Bogen
Lawrence Livermore National Laboratory
Livermore, CA

ABSTRACT

Multistage cancer risk models that account for clonal growth of intermediate, premalignant cell populations have been successfully used to describe age-specific incidence trends for human and experimentally induced animal tumors. Currently there is keen and growing interest in applying "cell-kinetic multistage" (CKM) models, which distinguish between mutations and cell population kinetics as separate processes influencing the rate of tumor formation, to the problem of predicting human cancer risk that may be posed by environmental agents. This paper illustrates the application of such models to cancer risk prediction for carbon tetrachloride (CCl_4), taking into account rodent cancer-bioassay data and CCl_4 pharmacokinetics in rodents and humans. The increased importance of knowledge concerning exposure scenarios when using CKM models for risk extrapolation, as opposed to more traditional approaches, is illustrated. The presumption, made in most CKM models considered to date, that preneoplastic cell growth is exponential over time, is critically evaluated along with the impact on predicted CCl_4-induced cancer risk of using a more biologically realistic cell-growth model. Because the potential application of CKM models to cancer risk prediction could have important consequences on public health measures directed at controlling environmental exposure to chemicals, the biological plausibility of specific CKM models considered for application deserves renewed scrutiny.

KEYWORDS: Carbon tetrachloride (CCl_4), cell-kinetic multistage (CKM) models, pharmacokinetic (PBPK) models, cancer-risk extrapolation

INTRODUCTION

Multistage cancer-risk models that account for clonal growth of intermediate (initiated, premalignant) cell populations, or "cell-kinetic multistage" (CKM) models, have long been successfully used to describe age-specific incidence trends for human cancer and experimentally induced tumors in animals.[1-3] More recently, a 2-stage stochastic model allowing for birth and death of initial and intermediate cells has been used to model human-cancer incidence in particular and has been proposed to be capable of describing spontaneous and induced carcinogenesis in general.[4-6] Currently there is keen and growing interest in the possibility of applying this 2-stage model to the problem of predicting the human cancer risk posed by environmental agents.[7-11] Because CKM models distinguish between mutations and cell-population kinetics as separate processes that influence the rate

Risk Analysis, Edited by C. Zervos
Plenum Press, New York, 1991

PM3006451723

Source: https://www.industrydocuments.ucsf.edu/docs/hkxj0001

of tumor formation, such models can predict widely different cancer risks for agents affecting only one process (e.g., promotion via induced cell proliferation, assuming a dose-response threshold) but not the other (e.g., mutagenesis, assuming a no-threshold dose-response relationship). Such an approach allows for distinct treatment of genotoxic carcinogens and nongenotoxic tumor promoters, provided the latter can be operationally defined. This approach has been advocated[11-13] but has not yet been incorporated into widely used cancer-risk-assessment procedures.[14,15]

This paper illustrates issues involved in the application of CKM models, in conjunction with physiologically based pharmacokinetic (PBPK) models, to the problem of cancer-risk extrapolation for the case of CCl_4 using the following approach. Appropriate PBPK models for predicting effective dose in rodents and humans as a function of CCl_4 exposure are first identified. It is presumed here that CCl_4 is not effective in producing mutations assumed (by the CKM approach) to be necessary to the carcinogenic process, but that CCl_4 is an effective "promoter" by virtue of an ability, at cytotoxic doses, to selectively increase the rate of net cell growth within premalignant cell clones. Hence, an appropriate model is fit to rodent data on the dose-response relationship for CCl_4-induced cell proliferation. This dose-response relationship is assumed to be the same for humans. An increase in cell proliferation is then presumed to correspond to a proportional increase in the value of the growth parameter of a 2-stage CKM model fit to a rodent-bioassay data set on increased cancer risk above background associated with different effective CCl_4 doses, which in turn correspond (using the rodent PBPK model) to the exposure scenario used in the bioassay selected as the basis for risk extrapolation.

Increased risk to humans associated with a given effective CCl_4 dose is then either presumed to be identical to predicted increased risk to rodents or calculated by fitting a corresponding 2-stage CKM model to human incidence data for cancer of the same type observed to be significantly increased in the selected rodent bioassay. These predicted relationships between effective dose and cancer risk are then transformed into corresponding relationships between human exposure and cancer risk using an appropriate human PBPK model and a scenario for human exposure to CCl_4 in drinking water. Because almost all CKM models considered to date have assumed that premalignant cells may proliferate exponentially over time *in vivo*, this paper also examines the implications of using an alternative, perhaps more biologically reasonable, assumption[16] that such cells grow geometrically over time. Finally, a comparison is made between the "virtually safe dose" (corresponding to a lifetime cancer risk of 10^{-6}) predicted using the CKM/PBPK approach illustrated here and that predicted using the more conservative approach typical in regulatory cancer-risk assessment.

DATA ON CCl_4-INDUCED CARCINOGENICITY IN RODENTS

Experimentally induced carcinogenic effects of CCl_4 observed in mice, rats and hamsters have led scientific and regulatory bodies to consider this compound a probable human carcinogen.[17-19] Dose-response data on induced cell proliferation (see below) are only available for mice. Therefore, cancer-risk extrapolation for the present analysis will be based on cancer-bioassay data derived from studies on mice by the National Cancer Institute (NCI). In particular, data will be used from the NCI studies[20-22] of female B6C3F1 mice weighing about 28 g that received 0, 1250, and 2500 mg/kg-d of CCl_4, 5 days/wk for 78 wk, by oral gavage using a corn-oil vehicle. Dosing began at 7 wk of age and surviving mice were observed up to 14 wk after dosing was stopped. Hepatocellular carcinomas were observed in one of the 80 pooled control female mice, 40 of the 40 low-dose mice, and 43 of the 45 high-dose mice.

Because 100% incidence was observed in the low-dose mice, these data cannot be used directly to derive a traditional estimate of hepatocarcinogenic potency for CCl_4 in

PM3006451724

Source: https://www.industrydocuments.ucsf.edu/docs/hkxj0001

mice. Nevertheless, the data indicate that a dose of 35 mg CCl_4 per animal on the NCI dosing regimen yielded a cumulative risk of liver cancer greater than (40-1)/40 or 97.5% by 97 wk of age in these mice. The value of >97.5% is used as a lower bound on incidence rate in the analysis below.

PBPK MODELS

The PBPK model of Paustenbach *et al.*[23] was adapted to estimate uptake and metabolism of CCl_4 in mice and humans in the present study. Here, CCl_4 metabolism in rats was assumed to be described by a single saturable pathway with V_{max} equal to 0.40 mg/hr-kg or, equivalently (by the body-weight scaling approach used here and described by Paustenbach *et al.*[23]) 0.14 mg/hr for a 225-g rat (the value empirically determined[24,25] for rats cited, but then not used for simulation purposes[23]). Corresponding scaled V_{max} values used here for modeling 30-g mice and 70-kg humans are 0.034 mg/hr and 7.78 mg/hr, respectively. The present analysis makes use of the partition coefficients for rats and humans used by Paustenbach *et al.*[23] and assumes that mice have the same partition coefficients as the rats of the latter model. All other physiological parameter values for 25-g mice and 70-kg humans were taken to be the reference values reported by the U.S. Environmental Protection Agency (U.S. EPA),[26] except that the latter reported human alveolar ventilation rate was increased from 5.0 to a more realistic 5.6 liters/hr. Numerical implementation of the model was done as previously described.[27,28] Other details and the results of PBPK analyses undertaken are described in the following sections.

A study[29] of the absorption kinetics of four chlorinated organic compounds administered by a single gavage dose to rats in aqueous and corn oil vehicles demonstrated that, over a 5-hr observation period, a corn oil vehicle decreases the rate and extent of uptake of these compounds relative to that observed using an aqueous vehicle; the greatest decrease in uptake observed was for trichloroethylene, the least water-soluble compound tested. For the present analysis, oral absorption kinetics for CCl_4 were presumed to be similar to those observed[29] for trichloroethylene administered in 10 mL/kg of corn oil to 400-g Wistar rats, which yielded a roughly constant, 90-min absorptive pulse of equivalent to a clearance of compound from the vehicle at a rate of about 0.11 mL vehicle/kg-min. The resulting total dose was about one 170th of that obtained using an aqueous vehicle (which, in turn, was assumed to be 100% of the administered dose). The vehicle-clearance rate of 0.11 mL/kg-min used here was assumed to scale to the −0.26 power of body weight[27] and to apply only to single-dose exposure scenarios. The effect of using a corn oil vehicle on absorption efficiency of chronically administered oral doses of similar compounds is currently unknown.

DOSE-RESPONSE FOR INDUCED CELL PROLIFERATION

Dose-response data on CCl_4-induced hepatocellular proliferation in 30-g male CD-1 mice were obtained from a recent study by Doolittle *et al.*[30] The mice in this study were given single (or daily) oral doses of from 0 to 100 mg/kg CCl_4 in 10 mL/kg corn oil, and measurements were made of the percent of hepatocytes in S-phase (%S) 48 hr after dosing and the concentration of selected enzymes in blood serum at various times after dosing. To estimate metabolized doses corresponding to the applied doses used in this study, one 170th of the ingested CCl_4 was assumed to be cleared from the corn oil vehicle at the constant rate of 0.22 mL/kg-min, yielding a 45-min pulse injected into the liver compartment (see discussion above). The results of the PBPK analysis scaled to apply to the mice used by Doolittle *et al.* are shown in Fig.1a.

Studies of rats exposed to CCl_4 by gavage have demonstrated that metabolism of this compound is the cause of its hepatotoxicity in rats.[31-34] One recent study further

PM3006451725

Source: https://www.industrydocuments.ucsf.edu/docs/hkxj0001

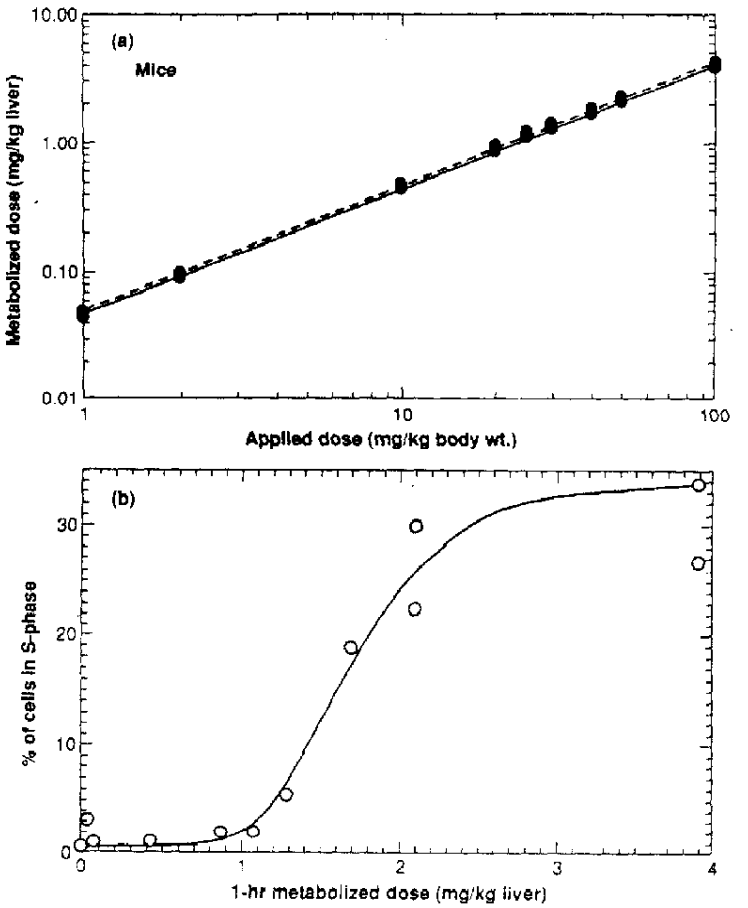

Fig. 1. (a) Metabolized dose as a function of orally administered dose of CCl_4 in corn oil to 30-g mice, based on the physiologically based pharmacokinetic model of Paustenbach *et al.*[23] modified and parameterized as explained in the text. Solid and dashed curves represent 1-hr and 24-hr total metabolized doses, respectively. Solid points indicate the administered doses used in the study by Doolittle *et al.*[30] referred to in the text. (b) Data (open circles) of Doolittle *et al.*[30] on the percent of hepatocytes in S-phase 48 hr after a single gavage dose (or in some cases the first of daily doses) of CCl_4 in corn oil to rats, as a function of the corresponding presumed effective (1-hr total metabolized) dose derived from (a) above. Solid curve is the function given by Eq. (1) in the text, fit to the data by least-squares optimization.

demonstrated that rats primarily metabolize CCl_4 to CO_2 and found that the rate of CO_2 production within 1 hr of dosing was the measure of CCl_4 metabolism most highly correlated (R^2=0.88) with the observed degree of liver injury as measured by elevation in serum glutamate-pyruvate transaminase (SGPT) concentration.[35] It was therefore assumed, for the present analysis, that the total amount of CCl_4 metabolized in 1 hr is the most appropriate metric of effective dose, d, for the cytotoxic effects observed by Doolittle *et al.*

The relationship between estimated values of d (from Fig. 1a) and the corresponding values of %S observed by Doolittle *et al.* is shown in Fig. 1b. Also shown is the log-normal dose-response model

$$\%S_d = \frac{100\%}{3}\,\Phi\left(\frac{\log_{10}(d) - a}{b}\right) + \%S_0\ , \qquad (1)$$

PM3006451726

Source: https://www.industrydocuments.ucsf.edu/docs/hkxj0001

in which Φ is the cumulative normal distribution function, $\%S_0$ is the background level of %S (0.5% in the mice studied), and d is 1-hr metabolized dose. The model was fit to the data shown using least-squares optimization of the location and shape parameters a and b (yielding best-fit values of 0.23 and 0.13 mg/kg-hr, respectively). This dose-response function for CCl_4-induced cell proliferation is a quasi-threshold model, based on the assumption that such proliferation represents regenerative cell growth following necrosis caused by acute toxicity of a sufficiently high dose of CCl_4. The factor of 100%/3 in the model accounts for the fact that %S was measured by Doolittle *et al.* as a fraction of total hepatocytes undergoing replicative DNA synthesis at 48 hr post exposure, whereas not all hepatocytes induced into S-phase are involved in synthesis precisely at that time. Clearly, a synchronous induction of 100% of hepatocytes into S-phase would be lethal. Detailed experiments have shown that CCl_4 intoxication or partial hepatectomy induces in rats and mice a wave of regenerative hepatocellular proliferation corresponding to an S-phase pulse commencing between 24 and 48 hr after administration and persisting between approximately 24 and 36 hr.[36-39] In fact, such proliferative response kinetics have been shown to be quite heterogeneous within rat liver, with hepatocytes in most liver zones reaching maximum %S values of between 20 and 35% at various times post injury.[37-38] This is consistent with the estimated upper bound of 33.3% for %S used in Eq. (1), based on an average S-phase duration of about 8 hr (in rats)[38] and an average duration of sustained induced peak S-phase activity of approximately 24 hr.[36-39]

The Doolittle *et al.* study included some investigation of how chronic (daily) dosing affects %S and serum enzyme levels in mice as compared to single dosing. Their results indicate that %S is lower with daily as opposed to single CCl_4 dosing by a factor of 2 to 3.[30] For the present analysis, it was therefore assumed that the factor 100%/3 in Eq. (1) must be replaced by 100%/9 when this model is applied to chronic dosing situations. The latter assumption implies that no chronic effective dose, regardless of its magnitude, would produce a value of %S greater than 11.6%.

An analysis of the Doolittle *et al.* data on CCl_4-induced increases in %S and 24-hr SGPT concentration (Fig. 2) shows that the correlation between these two indices of hepatotoxicity may be sufficient to enable increased SGPT to be used as a quantitative predictor of increased %S according to the relation

$$\%S_d = c\left[\log_{10}\left(\frac{\mathrm{SGPT}_d}{\mathrm{SGPT}_0}\right)\right] + \%S_0 \ , \qquad (2)$$

in which the slope constant c is equal to 10.9%. Figs. 3a-3c summarize an investigation of this hypothesis using data on induced changes in SGPT levels in male 225-g rats given single oral doses of CCl_4 in 2.5 mL/kg corn oil from a study by Reynolds *et al.*[35] The PBPK analysis for this study (Fig. 3a) assumed that one 170th of the ingested CCl_4 was cleared from the corn oil vehicle at a rate of 0.13 mL/kg-min, yielding a 19-min pulse injected into the liver compartment (see discussion above). The relation shown in Fig. 2 was then used to derive predicted %S values corresponding to observed elevations in SGPT at the estimated effective doses of CCl_4 to rats for the Reynolds *et al.* study. Eq. (1) was then fit to these predicted %S values as a function of effective dose as described above, yielding the parameter estimates a=0.93 and b=0.12 mg/kg-hr corresponding to the dashed curve shown in Fig. 3b, where this fit is compared to the one pertaining to mice from Fig. 1b. Fig. 3c shows that the dose-response models fit to the mouse data and the estimated rat data on elevated %S are approximately identical only if a from Eq. (1) for mice is assumed to increase by a factor of 5 and if c from Eq. (2) is assumed for rats to be 5.45 (i.e., half the value referred to above pertaining to mice). The first assumption suggests that the value of V_{max} for mice used in the PBPK analysis discussed above may be too low by a factor of 5, which is plausible in light of the fact that V_{max} for mice in this analysis was simply assumed to be identical to an estimate obtained for rats (i.e., mice may have a higher

PM3006451727

Source: https://www.industrydocuments.ucsf.edu/docs/hkxj0001

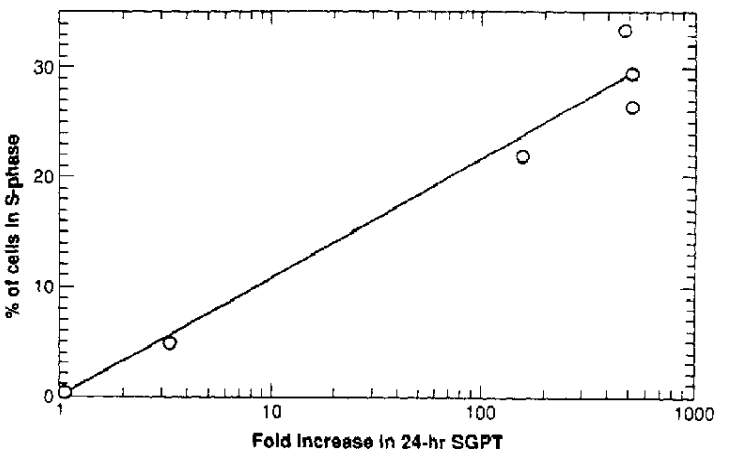

Fig. 2. Data (open circles) of Doolittle *et al.*[30] on percent of hepatocytes in S-phase (%S) 48 hr after gavage administration of various doses of CCl_4 in corn oil to 30-g mice, as a function of the fold increase (F) in SGPT concentration observed in these mice 24 hr after dosing. Solid line is the function given by Eq. (2) in the text, fit to the data by log-linear least-squares optimization.

capacity to metabolize CCl_4 than would be expected based simply on allometric scaling from an experimentally based estimate for rats). The second assumption suggests that the relation indicated by Eq. (2) and Fig. (2) may be species-specific.

CKM MODELS APPLIED TO CANCER LIVER DATA FOR MICE

The simple 2-stage CKM models used in the present analysis are described elsewhere[16] and are reviewed in the Appendix. Specifically, the exponential and geometric CKM models used here to predict cumulative cancer risk, R, as a function of age (minus a latency period here assumed to be 0) for a constant, lifetime exposure scenario, incorporate Eqs. (E-3) and (G-3) in the Appendix, where these are replaced by Eqs. (E-8) and (G-8), respectively, for scenarios involving n distinct exposure periods (i.e., in cases involving a sequence of n sets of parameter values governing mutation and cell proliferation rates). Because the NCI bioassays for CCl_4[20-22] involved preexposure, exposure, and postexposure periods (see discussion above), Eqs. (E-8) and (G-8) were used with n set equal to 3 to model hepatocellular cancer risk to the mice used. The cell-growth parameters of these models, g and a respectively (see Appendix), were fit to each of the single data points R_0=0.0125 and R_d=0.975 for the exposure scenario described above under the assumption that CCl_4 is a "pure promoter," i.e., acts only to increase the proliferation rate of initiated cells. Here, d is the effective (1-hr total metabolized) dose to liver tissue for NCI bioassay mice, estimated to be 21.1 mg/kg liver using the PBPK model described above, scaled to 28-g mice under the assumption that 100% of the chronically applied doses were absorbed. (Note that since 100% of these mice got liver cancer, R_d>0.975 so the corresponding models actually describe a plausible lower bound on true risk. Fig. 1b suggests that a similar response would have occurred had the effective dose been up to about 10 times less than it was.) To fit these models, it was also assumed that the NCI mice had 1.5×10^8 hepatocytes/g liver tissue[40] at risk throughout their lives of which roughly 25% were diploid cells at risk for malignant transformation,[41] yielding a total of 6×10^7 cells for 28-g mice with 5.5% liver tissue by weight, and that the two interstage mutation rates were each equal to 10^{-7}. The growth parameter values predicting the risks R_0 and R_d, $\{g_0, g_d\}$ and $\{a_0, a_d\}$ for the geometric and exponential CKM models respectively, produce the CKM functions shown in Fig. 4a.

PM3006451728

Source: https://www.industrydocuments.ucsf.edu/docs/hkxj0001

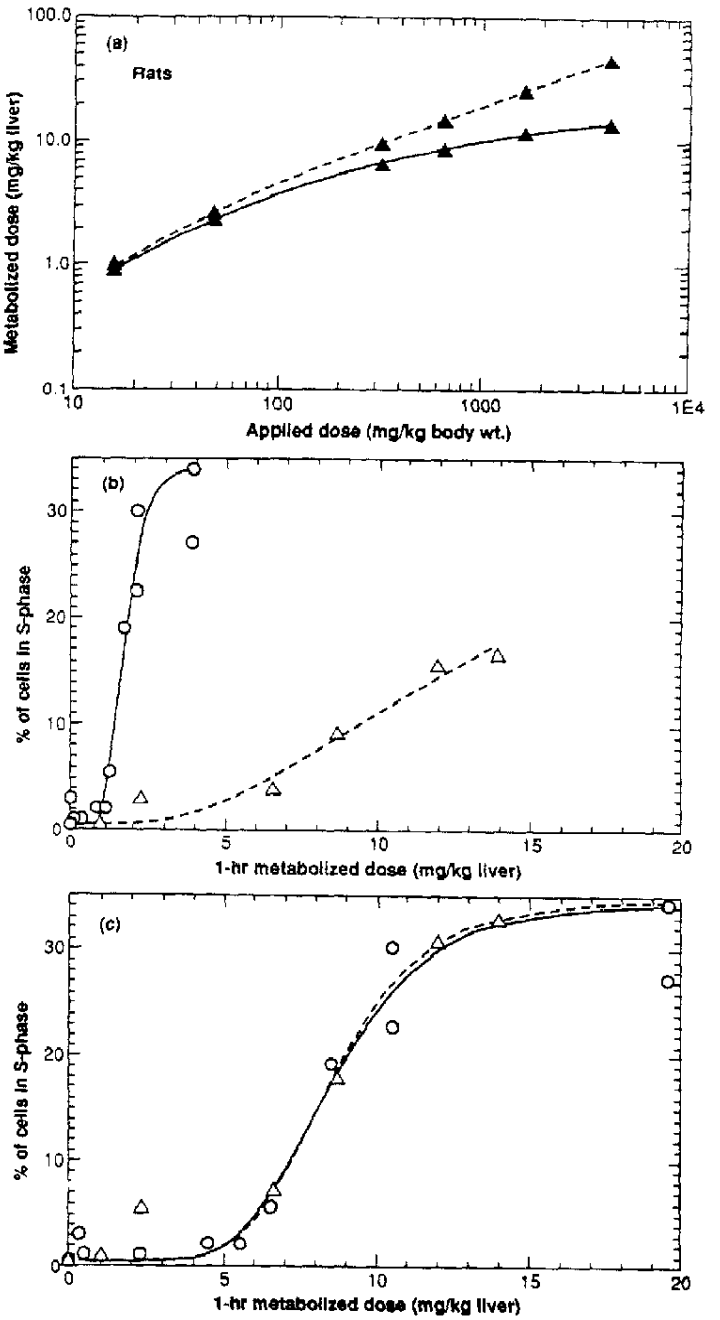

Fig. 3. (a) Metabolized dose as a function of orally administered dose of CCl_4 in corn oil to 225-g rats, based on the PBPK model of Paustenbach *et al.*[23] as explained in text. Solid and dashed curves represent 1-hr and 24-hr total metabolized doses, respectively; solid triangles indicate administered doses used in the Reynolds *et al.*[35] study. (b) Open triangles represent the predicted % in S-phase 48 hr after single gavage doses of CCl_4 in corn oil to rats extrapolated from Fig. 2 and from (a), using Eq. (1) from text; solid curve and associated data points redrawn from Fig. 1(b) for comparison. (c) The two curves in (b) converge if parameters are changed as explained in text.

PM3006451729

Source: https://www.industrydocuments.ucsf.edu/docs/hkxj0001

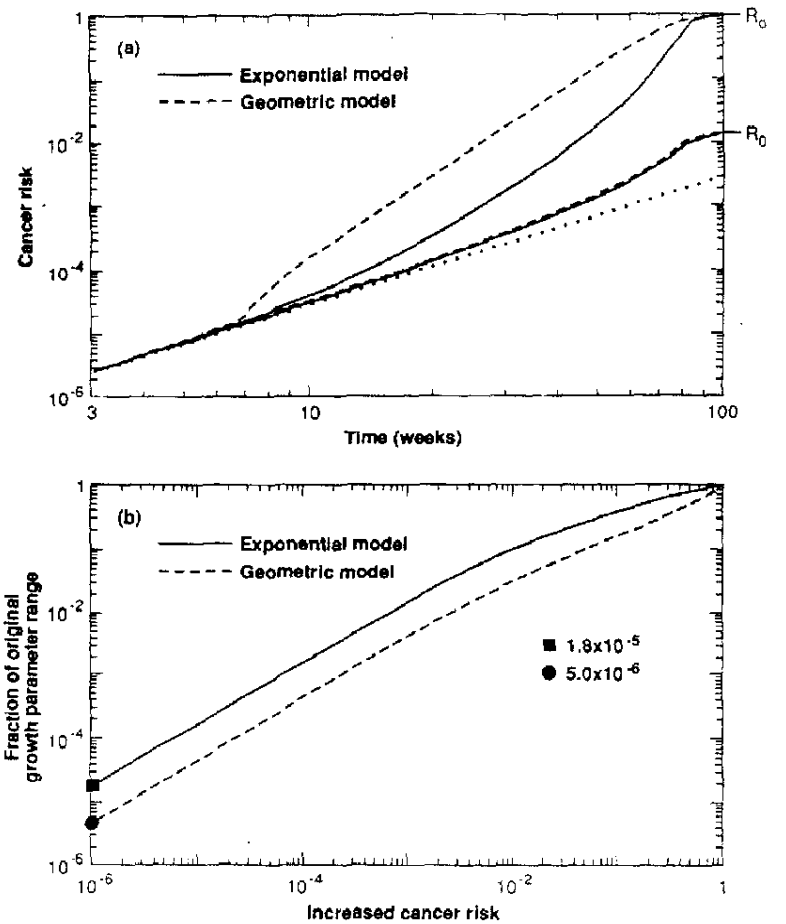

Fig. 4. Exponential and geometric cell-kinetic multistage models fit to tumor response data[20-22] for female mice exposed to CCl_4. (**a**) Solid and dashed curves are the functions 1-exp(E) and 1-exp(G), respectively, where E and G are given by Eqs. (E-3) and (G-3) in the Appendix, respectively, for which the constant $X_0 m_1 M_1$ is set to 6×10^{-7}. The functions are fit to the points R_0=0.0125 and R_d=0.975 at 97 wk, yielding the fitted exponential and geometric growth parameter values of $\{g_0=1.91, g_d=6.54\}$ and $\{a_0=0.939$ and $a_d=12.7\}$, respectively. The dotted line represents both models if the growth parameter is taken to be 0. (**b**) The fraction f corresponding to the growth parameter $z = z_0+f(z_d-z_0)$ (where z is either g or a) used in the models from (a) to predict a given risk R, as a function of increased risk $(R-R_0)/(1-R_d)$ for $R_0 \le R \le R_d$.

To proceed in the analysis, the background risk R_0 was assumed to be independent such that increased risk is defined as $A = (R-R_0)/(1-R_0)$, where $R_0 \le R \le R_d$, and that premalignant (stage-1) clones are resistant to the cytotoxicity of necrogenic doses of CCl_4, but are stimulated to proliferate to the same extent that surrounding normal hepatocytes are during regenerative growth following dosing.[42] It was further assumed that a change in %S by a given fraction f of its observed range corresponds to the same fractional change in net growth of premalignant cells, i.e., that

$$f = \frac{\%S - \%S_0}{\%S_d - \%S_0} = \frac{z - z_0}{z_d - z_0}, \qquad (3)$$

PM3006451730

Source: https://www.industrydocuments.ucsf.edu/docs/hkxj0001

where $0 \leq f \leq 1$ and where $z_0 \leq z \leq z_d$ for z equal to g or a. Thus, by decreasing f from 1 to 0, the curves leading to R_d in Fig. 4a are decreased until they converge to those leading to R_0. These assumptions and the information from Fig. 4a were then used to calculate f as a function of A for the exponential and geometric CKM models (Fig. 4b). Figure 4b shows that, based on the NCI mouse bioassay data, a reduction in f from 1 to between 5 and 20×10^{-6} is needed to ensure that $A=10^{-6}$.

CKM MODELS APPLIED TO LIVER CANCER DATA FOR HUMANS

The same approach taken above for using CKM models to describe liver cancer risk to the female NCI mice was applied to data on liver cancer incidence for human females. In this case, R_0 was taken to be 0.0005, the cumulative risk of getting liver cancer by age 75 for U.S. females during the period 1969-1971.[43] For humans receiving the same effective dose of CCl_4 that the NCI mice received, the corresponding lower bound on increased risk R_d was assumed to be approximately that applicable to the NCI mice. CKM models fit to each of these risk values are shown in Fig. 5a, and the corresponding relation of f to A shown in Fig. 5b demonstrates that, based on female liver cancer incidence data, a reduction in f from 1 to between 5 and 40×10^{-5} is needed to ensure that $A=10^{-6}$.

EXTRAPOLATION OF LIVER CANCER RISK TO HUMANS

Figure 6a shows effective dose as a function of f based on the data of Doolittle *et al.*[30] This relation was derived from Eq. (3) and the inverse of the relation specified in Eq. (1), appropriately modified to reflect a chronic dosing assumption. The analyses in the previous two sections indicate that, at minimum, a reduction in f from 1 to between 5 and 400×10^{-6} is needed to ensure that $A=10^{-6}$, which, in light of Fig. 6a, corresponds to an effective chronic CCl_4 dose rate of between 0.46 and 0.63 mg/kg liver per day. It was next assumed that this predicted range of "virtually safe" effective dose applies to humans as well as mice. To complete the analysis, a PBPK model for CCl_4-exposed 60-kg human females (with parameter values obtained as discussed above) was implemented using a chronic, daily scenario of ingestive exposure to CCl_4, e.g., in drinking water. Exposures were presumed to occur once per day, each modeled to result in a constant 6-min infusion of 100% of ingested CCl_4 into the liver compartment, and simulated exposures were repeated (for 7 simulated days) until dynamic equilibrium in effective (1-hr total metabolized) dose was approximated. The resulting relation of chronic applied to effective dose is shown in Fig. 6b. This information, combined with the previous analyses, leads to the prediction that an upper bound for the "virtually safe" dose rate of ingested CCl_4 for 60-kg humans is 3 to 5 mg/d, or 0.05 to 0.08 mg/kg-d, or 2 liters of water per day containing roughly 2 mg CCl_4 per liter. Recall that these represent upper bound figures because 100% of the low-dose NCI bioassay mice developed liver cancer.

DISCUSSION

The CKM-based approach to cancer risk assessment illustrated here for the case of CCl_4 differs fundamentally from more traditional risk assessment methods. Because the CKM model allows for a threshold-type dose response for agents considered to be "pure promoters," CKM-based risk estimates associated with exposure to such agents will typically be much lower than those based on "linear no-threshold" risk extrapolation methods. Using the latter methods, for example, the U.S. EPA[44] and the State of California[19,45] have, on the basis of animal cancer bioassay data such as the NCI study considered above, predicted a 10^{-6} (upper bound) increased cancer risk to be associated with ingestion of 4 sym(180) 10^{-6} and 5×10^{-5} mg/kg-d of CCl_4, respectively, which are from 3 to greater than 4 orders of magnitude lower than the corresponding upper bound

PM3006451731

Source: https://www.industrydocuments.ucsf.edu/docs/hkxj0001

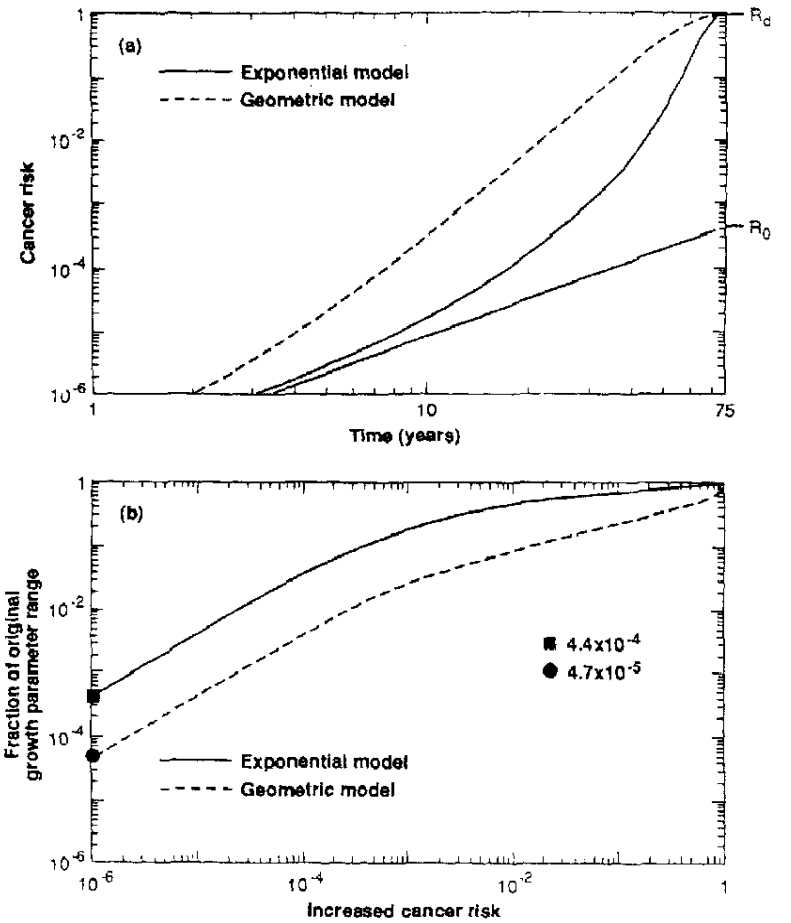

Fig. 5. Exponential and geometric cell-kinetic multistage models fit to the liver cancer incidence rate[43] (R_0=0.0005) for 75 yr-old U.S. females during 1969-1971 and to a much larger risk (R_d=0.987) presumed to be associated with a high-level, lifetime exposure to CCl_4. (a) Solid and dashed curves are the functions 1-exp(E) and 1-exp(G), respectively, where E and G are given by Eqs. (E-3) and (G-3) in the Appendix, respectively, for which the constant $X_0 m_1 M_1$ is set to 1.8×10^{-7} (the highest value possible to allow a fit to the risk values mentioned. The fitted exponential and geometric growth parameter values obtained are {g_0=0.0,g_d=0.181} and {a_0=0.0 and a_d=0.568}, respectively. (b) The fraction f corresponding to the growth parameter $z = z_0 + f(z_d - z_0)$ (where z is either g or a) used in the models from (a) to predict a given risk R, as a function of increased risk $(R-R_0)/(1-R_d)$ for $R_0 \leq R \leq R_d$.

"virtually safe" dose rates estimated above using the CKM-based approach. Even if a reduction in the latter values by 1 to 2 orders of magnitude is made to account for the 100% response in the NCI bioassay mice and for interindividual variability in humans, the CKM approach used here still predicts a much higher "safe" dose of CCl_4 than do the more traditional approaches.

It must be emphasized, however, that large uncertainties remain in defining the most appropriate way to implement CKM-based cancer risk extrapolation, even assuming the CKM approach is correct. The most fundamental source of uncertainty lies in the assumption made regarding the extent to which the observed carcinogenicity of a given

PM3006451732

Source: https://www.industrydocuments.ucsf.edu/docs/hkxj0001

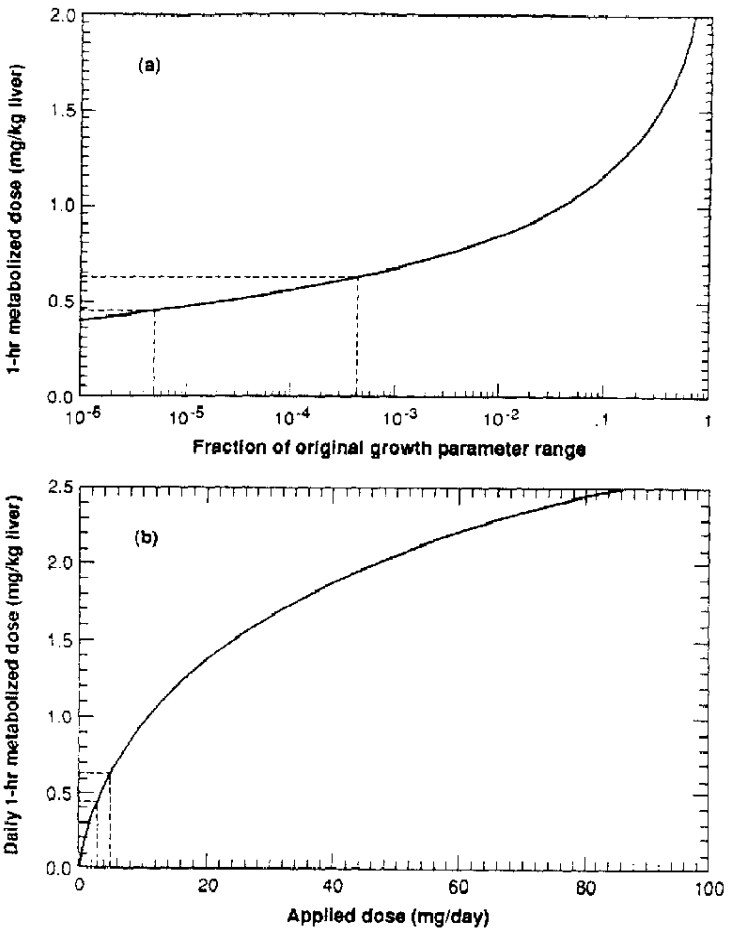

Fig. 6. (a) Predicted cytotoxically effective dose to mice as the function of f defined by Eq. (3) in the text, based on the inverse of the function specified by Eq. (1) in the text (in which the constant, 3, is replaced by 9 to account for the effect of chronic dosing). Dashed lines represent the range in values of f corresponding to a 10^{-6} risk from Figs. 4(b) and 5(b). (b) 1-hr total metabolized dose at dynamic equilibrium as a function of daily oral dose of CCl_4 to 60-kg humans, based on the physiologically based pharmacokinetic model of Paustenbach *et al.*[23] modified and parameterized as explained in the text. Dashed lines correspond to those in (a).

compound (say, in bioassay animals) is due to "promotion" (enhanced cell proliferation rates) alone, which reasonably can be presumed to have a threshold-type dose-response relationship, and how much is due to increased interstage transition rates (enhanced mutation rates), which is presumed by 2-stage CKM models to have a linear-quadratic dose-response relationship. Clearly, if a compound is assumed to have any degree of mutagenicity at all, this effect will ensure that the CKM dose-response relationship will be linear at sufficiently low doses.[46] The analysis above assumed that CCl_4 is a "pure promoter," which, despite the very limited evidence for CCl_4-induced genotoxicity *in vivo*,[44] may not strictly be the case. Other sources of uncertainty in this analysis include the effects of corn oil vehicle and chronic dosing on ingestive uptake of CCl_4 (sources not specific to CKM modeling), the selection of the most appropriate form of CKM model to use, and the quantitative relationship between changes in %S (or in SGPT levels) and changes in proliferation (birth minus death) rates in premalignant cells.

PM3006451733

Source: https://www.industrydocuments.ucsf.edu/docs/hkxj0001

Despite these uncertainties, the CKM approach incorporates the emerging facts regarding carcinogenesis to a far greater extent than do the more traditional risk extrapolation models. Thus, even when data available to implement a CKM-based risk extrapolation for a given compound are limited, consideration of this approach may provide heuristic advantages. For example, the present application to CCl_4 suggests that levels of serum enzymes (such as SGPT) associated with cytotoxicity and/or induced cell proliferation be routinely collected from animals during cancer bioassays, and that application of linear or quasi-linear risk extrapolation methods to data obtained from such bioassays be ruled out for those dose groups exhibiting significantly elevated levels of such enzymes.

ACKNOWLEDGMENTS

This work was performed under the auspices of the U.S. Department of Energy at the Lawrence Livermore National Laboratory with funds provided by the State of California, Department of Health Services, and the U.S. Air Force, H.G. Armstrong Aerospace Medical Research Laboratory, Toxic Hazards Division.

REFERENCES

1. P. Armitage and R. Doll, A Two-Stage Theory of Carcinogenesis in Relation to the Age Distribution of Human Cancer, *Br. J. Cancer* **11**:161-169 (1957).
2. P. Armitage and R. Doll, Stochastic Models for Carcinogenesis, Fourth Berkeley Symposium on Mathematics, Statistics, and Probability, pp. 19-38, University of California Press, Berkeley, CA (1961).
3. A. Whittemore and J. B. Keller, Quantitative Theories of Carcinogenesis, *SIAM Rev.* **20**:1-30 (1978).
4. S. H. Moolgavkar and D. J. Venzon, Two-Event Models for Carcinogenesis: Incidence Curves for Childhood and Adult Tumors, *Math. Biosci.* **47**:55-77 (1979).
5. S. H. Moolgavkar, N. E. Day, and R. G. Stevens, Two-Stage Model for Carcinogenesis: Epidemiology of Breast Cancer in Females, *J. Natl. Cancer Inst.* **65**:559-569 (1980).
6. S. H. Moolgavkar and A. G. Knudson, Mutation and Cancer: A Model for Human Carcinogenesis, *J. Natl. Cancer Inst.* **66**:1037-1052 (1981).
7. S. H. Moolgavkar, Model for Human Carcinogenesis: Action of Environmental Agents, *Environ. Health Perspect.* **50**:285-291 (1983).
8. T. W. Thorslund, C. C. Brown, and G. Charnley, Biologically Motivated Cancer Risk Models, *Risk Analysis* **7**:109-119 (1987).
9. J. A. Swenberg, F. C. Richardson, J. A. Boucheron *et al.*, High- to Low-dose Extrapolation: Critical Determinants Involved in the Dose Response of Carcinogenic Substances, *Environ. Health Perspect.* **76**:57-63 (1987).
10. S. H. Moolgavkar, A. Dewanji, and D. J. Venzon, A Stochastic Two-Stage Model for Cancer Risk Assessment. I. The Hazard Function and the Probability of Tumor, *Risk Analysis* **8**:383-392 (1988).
11. J. D. Wilson, Risk Assessment Reappraisals, [Letter] *Science* **240**:1126 (1988).
12. J. H. Weisburger and G. M. Williams, The Distinct Health Risk Analyses Required for Genotoxic Carcinogens and Promoting Agents, *Environ. Health Perspect.* **50**:233-245 (1983).
13. G. M. Williams, Definition of a Human Cancer Hazard, in *Nongenotoxic Mechanisms in Carcinogenesis (Banbury Report 25)*, pp. 367-380, B. E. Butterworth and T. J. Slaga, eds., Cold Spring Harbor Laboratory, Cold Spring Harbor, NY (1967).

PM3006451734

Source: https://www.industrydocuments.ucsf.edu/docs/hkxj0001

14. E. L. Anderson and the Carcinogen Assessment Group of the U.S. Environmental Protection Agency, Quantitative Approaches in Use to Assess Cancer Risk, *Risk Analysis* **5**:277-295 (1985).
15. U.S. Environmental Protection Agency (EPA), Guidelines for Carcinogen Risk Assessment, *Federal Register* **51**:33992-34003 (1986).
16. K. T. Bogen, Cell Proliferation Kinetics and Multistage Cancer Risk Models, *J. Natl. Cancer Inst.* **81**:267-277 (1989).
17. U.S. Environmental Protection Agency (EPA), Health Assessment Document for Carbon Tetrachloride, EPA-600/8-82-001F, U.S. EPA Environmental Criteria and Assessment Office, Cincinnati, OH (1984).
18. IARC, International Agency for Research on Cancer, Some Halogenated Hydrocarbons, *IARC Monographs on the Evaluation of Carcinogenic Risk of Chemicals to Man* **20**:371-399 (1979).
19. N. R. Reed, R. Babapour, W. Reed, L. Beltran, and D. P. H. Hsieh, Health Risk Assessment of Carbon Tetrachloride in California Drinking Water, Report prepared for the California Public Health Foundation on behalf of the California Department of Health Services, Department of Environmental Toxicology, University of California, Davis, CA (1988).
20. National Cancer Institute (NCI), Report on the Carcinogenesis Bioassay of Chloroform, Carcinogenesis Program, Division of Cancer Cause and Prevention (1976).
21. National Cancer Institute (NCI), Report on the Carcinogenesis Bioassay of Trichloroethylene, National Cancer Institute Technical Report Series, No. 2, NCI-CG-TR-2 (1976).
22. National Cancer Institute (NCI), Bioassay of 1,1,1-Trichloroethane for Possible Carcinogenicity, National Cancer Institute Technical Report Series, No. 3, NCI-CG-TR-3 (1976).
23. D. J. Paustenbach, H. J. Clewll, III, M. L. Gargas, and M. E. Andersen, A Physiologically-Based Pharmacokinetic Model for Inhaled Carbon Tetrachloride, *Toxicol. Applied Pharmacol.* **96**:191-211 (1988).
24. M. L. Gargas, P. G. Seybold, and M. E. Andersen, Modeling the Tissue Solubilities and Metabolic Rate Constant (V_{max}) of Halogenated Methanes, Ethanes, and Ethylenes, *Toxicol. Letters* **43**:235-256 (1988).
25. M. L. Gargas, M. E. Andersen, and H. J. Clewell, III, A Physiologically Based Simulation Approach for Determining Metabolic Constants from Gas Uptake Data, *Toxicol. Appl. Pharmacol.* **86**:341-352 (1988).
26. U.S. Environmental Protection Agency (EPA), Reference Physiological Parameters in Pharmacokinetic Modeling, EPA-600/6-88/004, NTIS PB88-196019, U.S. EPA Office Research and Development, Office of Health and Environmental Assessment, Washington, DC (1988).
27. K. T. Bogen, Pharmacokinetics for Regulatory Risk Analysis: The Case of Trichloroethylene, *Regulatory Toxicol. Pharmacol.* **8**:447-466 (1988).
28. K. T. Bogen and L. H. Hall, Pharmacokinetics for Regulatory Risk Analysis: The Case of 1,1,1-Trichloroethane (Methyl Chloroform), *Regulatory Toxicol. Pharmacol.* **10**:26-50 (1989).
29. J. R. Withey, B. T. Collins, and P. G. Collins, Effect of Vehicle on the Pharmacokinetics and Uptake of Four Halogenated Hydrocarbons from the Gastrointestinal Tract of the Rat, *J. Appl. Toxicol.* **3**:249-253 (1983).
30. D. J. Doolittle, G. Muller, and H. E. Scribner, Relationship Between Hepatotoxicity and Induction of Replicative DNA Synthesis Following Single or Multiple Doses of Carbon Tetrachloride, *J. Toxicol. Environ. Health* **22**:63-78 (1987).
31. J. V. Bruckner, W. F. MacKenzie, S. Muralidhara, R. Luthra, G. M. Kyle, and D. Acosta, Oral Toxicity of Carbon Tetrachloride: Acute, Subacute, and Subchronic Studies in Rats, *Fundam. Appl. Toxicol.* **6**:16-34 (1986).
32. H. G. Shertzer, M. P. Niemi, F. A. Reitman, M. L. Berger, B. L. Myers, and M. W. Tabor, Protection Against Carbon Tetrachloride Hepatotoxicity by Pretreatment with Indole-3-carbinol, *Exp. Mol. Pathol.* **46**:180-189 (1987).

PM3006451735

Source: https://www.industrydocuments.ucsf.edu/docs/hkxj0001

33. G. Labbe, V. Descatoire, P. Letteron, C. Degott, M. Tinel, D. Larrey, Y. Carrion-Pavlov, J. G. G. Amouyal, and D. Pessayre, The Drug Methoxsalen a Suicide Substrate for Cytochrome P-450, *Biochem. Pharmacol.* **36**:907-914 (1987).
34. H. G. Shertzer, M. L. Berger, and M. W. Tabor, Intervention in Free Radical Mediated Hepatotoxicity and Lipid, *Biochem. Pharmacol.* 37:333-338 (1988).
35. E. S. Reynolds, R. J. Treinen, H. H. Farrish, and M. T. Moslen, Metabolism of [14C] Carbon Tetrachloride to Exhaled, Excreted and Bound Metabolites: Dose-Response, Time-Course and Pharmacokinetics, *Biochem. Pharmacol.* **33**:3363-3374 (1984).
36. C. M. Leevy, R. M. Hollister, R. Schmid, R. A. MacDonald, and C. S. Davidson, Liver Regeneration in Experimental Carbon Tetrachloride Intoxication, *Proc. Soc. Exp. Biol. Med.* **102**:672-675 (1959).
37. H. Gerhard, A Quantitative Model of Cellular Regeneration in Rat Liver After Partial Hepatectomy, in *Liver Regeneration after Experimental Injury: III Workshop on Experimental Liver Injury*, pp. 340-346, R. Lesch and W. Reutter, eds. Stratton Intercontinental Medical Book Corporation, NY (1973).
38. H. M. Rabes, H. V. Tuczek, and R. Wirsching, Kinetics of Hepatocellular Proliferation After Partial Hepatectomy as a Function of Structural and Biochemical Heterogeneity of the Rat Liver, in *Liver Regeneration after Experimental Injury: III Workshop on Experimental Liver Injury*, pp. 35-55, R. Lesch and W. Reutter, eds., Stratton Intercontinental Medical Book Corporation, NY (1973).
39. B. Schultze, H. Gerhard, and W. Maurer, A Quantitative Model of Liver Regeneration in the Mouse After CC14 Intoxication, in *Liver Regeneration after Experimental Injury: III Workshop on Experimental Liver Injury*, pp. 330-339, R. Lesch and W. Reutter, eds., Stratton Intercontinental Medical Book Corporation, NY (1973).
40. S. Petersen, Flow Cytometry of Human Colorectal Tumors: Nuclear Isolation by Detergent Technique, *Cytometry* **6**:452-460 (1985).
41. H. Danielsen, H. B. Steen, T. Lindmo, and A. Reith, Ploidy Distribution in Experimental Liver Carcinogenesis in Mice, *Carcinogenesis* **9**:59-63 (1988).
42. T. A. Dragani, G. Manenti, and G. D. Porta, Enhancing Effects of Carbon Tetrachloride in Mouse Hepatocarcinogenesis, *Cancer Lett.* **31**:171-179 (1986).
43. National Cancer Institute (NCI), Third National Cancer Survey: Incidence Data, National Cancer Institute Monograph 41, DHEW Publication No. NIH 75-787, p. 100, U.S. Department of Health, Education and Welfare, Bethesda, MD (1975).
44. U.S. Environmental Protection Agency (EPA), Health Assessment Document for Carbon Tetrachloride, EPA-600/8-82-001F, Environmental Criteria and Assessment Office, U.S. EPA, Cincinnati, OH (1984).
45. California Department of Health Services, Proposition 65 Risk-Specific Intake Levels: Carbon Tetrachloride, Draft report, Reproductive and Cancer Hazard Assessment Section, Office of Environmental Health Hazard Assessment (1988).
46. C. J. Portier, Statistical Properties of a Two-Stage Model of Carcinogenesis, *Environ. Health Perspect.* **76**:125-131 (1987).

APPENDIX

For cell-kinetic multistage (CKM) models in general,[16] the stage-j cell populations of a k-stage process of carcinogenesis are represented by the stochastic processes $X_j(T)$, $j=1,...,k$, over the period $0 \le t \le T$, where $X_j(0)=0$; $X_0(T)$ is a deterministic nonnegative (DN) ("driving") function; and $m_j(T)$, for $j=0,...,k-1$ and $m_j(T)T<<1$, are DN functions (stage-specific mutation rates) such that the probability of a unit gain by $X_{j+1}(T)$ caused by a simultaneous unit loss from $X_j(T)$ during the interval $[T,T+dT)$ is approximately $m_i(T)dT$, and the probability of more than one such event occurring in this interval is negligible. In semi-stochastic CKM models, $w_j(T)$, $j=1,...,k-1$, are DN impulse-response (or weighting) functions used to represent (premalignant) cell proliferation subsequent to the occurrence of

PM3006451736

Source: https://www.industrydocuments.ucsf.edu/docs/hkxj0001

each new stage-j clone arising by mutation of a stage-$(j-1)$ cell, where $w_k(T) = 1$. Finally, let $R(t) = \text{Prob}\{X_k(t) \geq 1\}$, i.e., $R(t)$ is the cumulative distribution of the waiting time for the occurrence by time t of the first increment in $X_k(t)$, representing the first cancer cell. It has been shown for semistochastic CKM models in general that $R(t) \approx EX_k(t)$ for $R(t)<<1$ and that $R(t) \approx 1-\exp(EX_k(t))$ is a first-order approximation for all $R(t)$, where E denotes the expectation operator.[16]

Derived below are the approximate solutions for 2-stage (i.e, k=2), semistochastic, exponential and geometric CKM models of carcinogenesis in the case that parameter values governing mutation rates and cell proliferation in intermediate-stage (here, in stage-1) cells change at times t_i for i=1,...,n, where t_0=0, $t_{i-1} \leq t_i$, and t_n=t. Here it is assumed that $X_0(T)$ is equal to the constant X_0 and that $m_j(t_{i-1} \leq T \leq t_i)$ for j=0 and j=1 are equal to the constants m_i and M_i, respectively. From these assumptions, it follows[16] that for both exponential and geometric CKM models,

$$EX_1(t_n) \approx \sum_{i=1}^{n} \int_{t_{i-1}}^{t_i} X_0 m_i w_1(t_i - T)dT \quad , \text{ and} \tag{A-1}$$

$$EX_2(t_n) \approx EX_2(t_{n-1}) + \int_{t_{n-1}}^{t_n} M_n EX_1(T)dT \quad . \tag{A-2}$$

In the following evaluations of Eqs. (A-1) and (A-2), the growth response function, $w_1(T)$, for all proliferating premalignant (i.e., stage-1) cells is taken to be a function of the growth parameter z, where z is designated g and a in exponential and geometric CKM models, respectively, and where z at time T equals the constant z_i for $t_{i-1} \leq T \leq t_i$, i=1,...,n. Also, p_i will be used to denote the vector $\{m_i, M_i, z_i\}$ of mutation- and growth-related parameter-values in operation over the period from t_{i-1} to t_i, i=1,...,n.

I. Exponential 2-Stage CKM Models

For 2-stage exponential CKM models, $w_1(T) = e^{gT}$ when n=1, so that Eqs. (A-1) and (A-2) yield

$$EX_1(t_1) \approx X_0 \frac{m_1}{g_1}\left(e^{g_1 t_1} - 1\right) \tag{E-1}$$

$$= EX_1(p_1, t_1) \quad , \text{ and} \tag{E-2}$$

$$EX_2(t_1) \approx X_0 \frac{m_1 M_1}{g_1^2}\left(e^{g_1 t_1} - g_1 t_1 - 1\right) \tag{E-3}$$

$$= EX_2(p_1, t_1) \quad . \tag{E-4}$$

To consider cases in which n>1, we first define

$$\epsilon_{r,s} = \begin{cases} \sum_{i=r}^{s} g_i(t_i - t_{i-1}) & \text{for } r \leq s \\ 0 & \text{for } r > s \end{cases} \tag{E-5}$$

and note that $w_1(T) = \exp(g_i T + \epsilon_{i+1,n})$ during the period t_{n-1} to t_n for stage-1 clones arising at time T where $t_{i-1} \leq T \leq t_i$. Upon substitution, Eqs. (A-1) and (A-2) yield

$$EX_1(t_n) \approx \sum_{i=1}^{n} \int_{t_{i-1}}^{t_i} X_0 m_i \exp(g_i(t_i - T) + \epsilon_{i+1,n})dT \quad , \tag{E-6}$$

PM3006451737

Source: https://www.industrydocuments.ucsf.edu/docs/hkxj0001

$$\approx \sum_{i=1}^{n} X_0 \frac{m_i}{g_i}\left[\exp(\epsilon_{i,n}) - \exp(\epsilon_{i+1,n})\right] \quad , \text{ and} \tag{E-7}$$

$$EX_2(t_n) \approx \sum_{i=1}^{n} EX_2(p_i, t_i - t_{i-1}) + \sum_{i<j\leq n}\left[X_0 \frac{m_i M_j}{g_i g_j}(\exp(\epsilon_{i,i} - 1))\right.$$
$$\left. \cdot (\exp(\epsilon_{j,j} - 1))\ \exp(\epsilon_{i+1,j-1})\right] \quad . \tag{E-8}$$

II. Geometric 2-Stage CKM Models

For 2-stage geometric CKM models in the case that n=1, it has been shown[16] that $w_1(T) = (aT+1)^x$ (where in the text x=3 to model premalignant clones assumed to grow spherically with radial growth proportional to time). For these geometric CKM models, Eqs. (A-1) and (A-2) yield

$$EX_1(t_1) \approx X_0 \frac{m_1}{(x+1)a_1}\left[\left(a_1 t_1 + 1\right)^{x+1} - 1\right] \tag{G-1}$$

$$= EX_1(p_1, t_1) \quad , \text{ and} \tag{G-2}$$

$$EX_2(t_1) \approx X_0 \frac{m_1 M_1}{(x+1)(x+2)a_1^2}\left[\left(a_1 t_1 + 1\right)^{x+2} - \left((x+2)a_1 t_1\right) + 1\right] \tag{G-3}$$

$$= EX_2(p_1, t_1) \quad . \tag{G-4}$$

To consider cases in which n>1, we first define

$$\gamma_{r,s} = \begin{cases} 1 + \sum_{i=r}^{s} a_i(t_i - t_{i-1}) & \text{for } r \leq s \\ 1 & \text{for } r > s \end{cases} \tag{G-5}$$

and note that $w_1(T) = (a_i T + \gamma_{i+1,n})^x$ during the period t_{n-1} to t_n for stage-1 clones arising at time T where $t_{i-1} \leq T \leq t_i$. Upon substitution, Eqs. (A-1) and (A-2) now yield

$$EX_1(t_n) \approx \sum_{i=1}^{n} \int_{t_{i-1}}^{t_i} X_0 m_i\left[\left(a_i(t_i - T) + \gamma_{i+1,n}\right)\right]^x dT \quad , \tag{G-6}$$

$$\approx \sum_{i=1}^{n} X_0 \frac{m_i}{(x+1)a_i}\left(\gamma_{i,n}^{x+1} - \gamma_{i+1,n}^{x+1}\right) \quad , \text{ and} \tag{G-7}$$

$$EX_2(t_n) \approx \sum_{i=1}^{n} EX_2(p_i, t_i - t_{i-1}) + \sum_{i<j\leq n}\left[X_0 \frac{m_i M_j}{(x+1)(x+2)a_i a_j}\right.$$
$$\left. \cdot \left(\gamma_{i,j}^{x+2} - \gamma_{i,j-1}^{x+2} - \gamma_{i+1,j}^{x+2} + \gamma_{i+1,j-1}^{x+2}\right)\right] \quad . \tag{G-8}$$

PM3006451738

Source: https://www.industrydocuments.ucsf.edu/docs/hkxj0001